MALAYSIAN JOURNAL OF ANALYTICAL SCIENCES

Journal homepage: https://mjas.analis.com.my/

Research Article

The potential of eggshell waste as an alternative filler in natural rubber composites

Abdulhakim Masa[1*], Chananchida Janpong[1], Anchuleekorn Kaomodjod[1], Sasipim Chatarat[1], Ruedee Jaratrotkamjorn[1], and Siriwat Soontaranon[2]

[1]Rubber Engineering Program, Department of Interdisciplinary Engineering, Faculty of Engineering, Prince of Songkla University, Hat Yai, Songkla 90110, Thailand
[2]Synchrotron Light Research Institute, Muang District, Nakhon Ratchasima 30000, Thailand

[*]Corresponding author: abdulhakim.m@psu.ac.th

Received: 26 December 2025; Revised: 18 April 2026; Accepted: 18 August 2026; Published: 31 October 2026

Abstract
This study assesses the applicability of eggshell waste powder as a calcium carbonate ($CaCO_3$) filler in natural rubber (NR) composites. A composite containing commercial-grade $CaCO_3$ was also prepared for reference. The effects of eggshell powder particle size on the NR's morphological, mechanical, thermomechanical, swelling, and processing-ability features were examined. The inclusion of eggshell powder improved the rubber composites' curing torque, swelling resistance, crosslink density, and modulus at different stresses when compared to an unfilled control sample, but it reduced their tensile strength, extensibility, and thermomechanical characteristics independent of particle size. In contrast, the commercial-grade $CaCO_3$ improved all properties due to greater interaction with the rubber matrix compared to the eggshell powder (ESP). The ability of NR to crystallize during stretching was reduced by adding $CaCO_3$ in all cases, so these fillers retard the strain-induced crystallization. The tensile strength of NR composites filled with ESP 132 decreased by 7.23% compared to that filled with commercial-grade $CaCO_3$, while a greater reduction of 33.87% was observed for the composite containing ESP 300. The mechanical properties remained acceptable, with tensile strength ~ 17.83 MPa and elongation at break ~ 394%, even though the inclusion of eggshell powder led to poor thermal properties. This happened when the eggshell powder with a particle size of 132 µm was utilized. Therefore, it would be practical to use eggshell waste as a filler in rubber-based goods. This bio-filler has substantial benefits in rubber formulations because of its sustainability and availability.

Keywords: natural rubber, composites, eggshell waste, calcium carbonate, filler

Introduction

Natural rubber (NR) is rarely used unless it is reinforced with fillers. Depending on the intended use, several kinds of fillers have been added to rubber. Some of them are added to enhance the final properties, while others are incorporated to aid in the rubber production and molding processes, and to reduce material costs [1,2,3].

One of the most significant white fillers is calcium carbonate ($CaCO_3$), which is frequently utilized in rubber goods [4]. $CaCO_3$ is frequently added to rubber composites as a filler to save costs, but it also improves their modulus, hardness, dimensional stability, and heat resistance [5]. Chicken eggshell, a byproduct from food processing and production, is an alternative source of $CaCO_3$ that might be utilized as filler in rubber formulations. Because eggshell waste is a renewable waste resource and has a high calcium carbonate concentration that is equivalent to traditional mineral fillers, there is interest in using it as a filler in rubber composites. The eggshell has been discovered to contain around 94% calcium carbonate ($CaCO_3$) as calcite, 1% magnesium carbonate, 1% calcium phosphate, and organic content, including proteins [3,6,7]. Generally, eggshell waste is disposed of in landfills without further treatment. This practice may cause other environmental problems, such as waste contamination, soil pollution, and other environmental hazards [8,9]. It would be better to handle this bio-waste properly. Chicken eggshell waste is an interesting option for filler in rubber composites because of its high $CaCO_3$ content. In addition to being a bio-filler, it is cheap, plentiful, and low-density, all of which are advantageous for a

variety of rubber goods [10]. Using eggshells as filler lowers the risk of environmental contamination and adds value to eggshell waste. The use of eggshell waste as a filler in rubber composites is of great importance as it might improve several of the composites' characteristics [3,6,7,8,11]. For instance, Intharapat et al. [6] investigated the potential of using chicken eggshell waste as a bio-filler in epoxidized NR composites. They found that eggshell filler enhanced the curing and the mechanical properties of these composites. This resulted from the eggshell filler's excellent dispersion and filler-rubber interaction. Barrera and Cornish [12] investigated the possibility of using eggshell filler as a partial replacement of carbon black. They discovered that when eggshell was added as a co-filler at low loadings (5 and 10 phr), the tensile results were similar to those of composites filled only with carbon black. Sowinska-Baranowska and Maciejewska [3] investigated improving the dispersion of eggshell filler and its interactions with the rubber matrix by using different compatibilizers. They discovered that using ionic liquids or cetyltrimethylammonium bromide as a compatibilizer improved the composites' tensile features. Eggshell filler decreased elongation at break but increased the composites' resilience to thermo-oxidative aging compared to the unfilled sample.

Although numerous studies have explored the application of waste eggshell powder as filler in the NR composites, a comprehensive understanding of its role, particularly in thermomechanical behavior and strain-induced crystallization, remains limited. This study addresses these gaps by elucidating the structure–property relationships governing eggshell-filled NR systems. Two particle sizes of eggshell powder were prepared via manual grinding using a mortar, followed by sieving before incorporation into NR. The properties of eggshell waste-filled NR composites were compared with those of NR composites filled with commercial-grade $CaCO_3$. A comprehensive evaluation encompassing curing characteristics, swelling behavior, morphological and mechanical properties, microstructural evolution during stretching, and thermomechanical performance was conducted to elucidate the role of eggshell filler. Finally, the use of eggshell waste as an effective and sustainable filler for NR composites was demonstrated.

Materials and Methods

Materials

The Standard Thai Rubber graded STR 5L, used as the rubber matrix, was supplied by Chalong Latex Industry Co. Ltd., Songkhla, Thailand. Curing activators, zinc oxide (ZnO) and stearic acid, were supplied by T.C. group Co., Ltd., Songkhla, Thailand, and Imperial Chemical Co., Ltd., Pathumthani, Thailand, respectively. Commercial-grade calcium carbonate (Omyacarb 1T-TN) was produced by Tetravion Ltd., Thessaloniki, Greece. It is a surface-treated fine powder with good dispersion capabilities and a mean particle size of approximately 2.1 μm [13]. Eggshell waste was kindly supplied by the Bakery shop, Trang, Thailand. The antioxidant, N-(1,3-dimethylbutyl)-N’-phenyl-p-phenylenediamine (6PPD), was manufactured by Eastman Chemical Company, Tennessee, United States. N-Tertiarybutyl-2-benzothaiazole sulfenamide (TBBS), used as a curing accelerator and the sulfur curing agent were supplied by Geefin Rubber Tech Co., Ltd., Songkhla, Thailand.

Eggshell powder preparation

Using the technique shown in **Figure 1**, two eggshell powder particle sizes were produced in-house. 1,000 grams of eggshell debris were repeatedly cleaned using tap water. The lighter eggshell membrane was separated from the heavier calcium carbonate by soaking it in 4.5 L of commercial distilled 5% vinegar for 30 minutes [14]. The remaining membrane was removed from the eggshell before it was dried in the sun for eight hours. Using a mortar, the dry eggshells were hand-crushed and ground into a fine powder. Eggshell powders with particle sizes of 132 μm (ESP 132) and 300 μm (ESP 300) were obtained by passing the powder through sieves of 120 mesh and 60 mesh, respectively. After that, the eggshell powders were stored in hygienic, sealed containers until they were needed. Note that the particle sizes of eggshell powder passing through 60- and 120-mesh sieves were converted to approximately 300 μm and 132 μm, respectively, using the mesh–particle size conversion table provided by the sieve supplier.

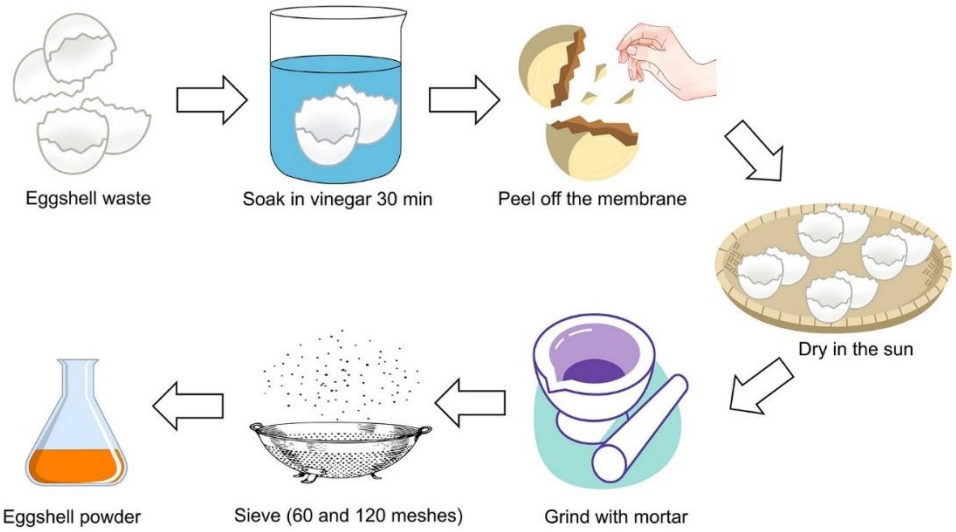


Figure 1. Preparation of eggshell powder

Rubber compound preparation

The compound formulations of rubber and other ingredients listed in Table 1 were prepared by using a laboratory-sized two-roll mill, model ML-D6L12 (Chareontut Co. Ltd, Samutprakarn, Thailand), at room temperature. The guide and nip were positioned at 15 cm and 1.2 mm, respectively. Before adding the ZnO and stearic acid, the STR 5L was masticated for three minutes. The filler (commercial-grade $CaCO_3$ or eggshell powder) was added after one minute and stirred for seven minutes. After that, the mixer was filled with 6PPD and allowed to mix for one minute. After adding the TBBS for one minute, the sulfur was finally introduced. All chemicals were mixed for a total of 14 minutes. The rubber compounds were then rolled for 6 times before sheeting. For baseline reference purposes, NR compounds without filler were also prepared using similar steps. The compounds were left overnight at room temperature. The resulting rubber compounds were vulcanized in a laboratory hydraulic pressing machine, Model SLLP30 (Siam Lab, Nonthaburi, Thailand) at 170 °C, following their respective curing times (t_{90}). The NR composites containing 30 phr ESP 132 and ESP 300 were named "ES - $CaCO_3$ 132" and "ES - $CaCO_3$ 300", while the composite filled with commercial-grade $CaCO_3$ was named "Ref - $CaCO_3$", and the sample free of filler is labeled "Control".

Characterizations

An X-ray fluorescence (XRF) spectrometer (Zetium, PANalytical, Netherlands) was used to analyze the chemical compositions of $CaCO_3$ substitutes. All samples were burnt using the thermal analyzer model STA8000 (Perkin Elmer, USA) before the XRF test. The information gathered from the XRF and thermal analyzer was documented.

The curing characteristics of all NR compounds, in terms of minimum and maximum torques (M_L and M_H), torque difference ($M_H - M_L$), scorch time (t_{s1}), cure time (t_{90}), and cure rate index (CRI), were characterized at 170 °C for 30 min by using a moving die rheometer (Montech MDR 3000 BASIC, Buchen, Germany).

Table 1. Formulations of the NR compounds (phr = parts per hundred parts of rubber)

Ingredient	Quantity (phr)			
	Control	**Ref - $CaCO_3$**	**ES - $CaCO_3$ 132**	**ES - $CaCO_3$ 300**
STR 5L	100	100	100	100
ZnO	3	3	3	3
Stearic acid	1	1	1	1
Commercial $CaCO_3$	0	30	-	-
ESP 132	0	-	30	-
ESP 300	0	-	-	30
6PPD	1	1	1	1
TBBS	1.5	1.5	1.5	1.5
Sulfur	1.5	1.5	1.5	1.5

Samples measuring 1 cm x 1 cm x 0.1 cm were submerged in 30 mL of toluene solvent at room temperature for 48 hours to conduct equilibrium swelling tests of the NR and its composites. The swelling degree was calculated as follows:

$$\text{Swelling degree (\%)} = \left(\frac{W_s\text{-W}_i}{W_i}\right) \quad (1)$$

where W_i is the initial weight of the sample (g) and W_s is the weight of the swollen sample (g).

Total crosslink density (ν) for all samples was calculated by applying the Flory-Rehner equation [15]:

$$\nu = \frac{1}{2M_c} = -\frac{ln(1-V_r)+V_r+\chi V_r^2}{2\rho V_s\left(V_r^{1/3}-\frac{V_r}{2}\right)} \quad (2)$$

where M_c refers to the average molecular weight between cross-links, V_r is the volume fraction of rubber in the swollen mass, χ is the polymer-solvent interaction parameter (0.39 for the NR-toluene system) [16], ρ is the density of the rubber, and V_s is the molar volume of the solvent (106.3 cm^3/mol). The V_r can be calculated as follows:

$$V_r = \frac{\frac{W_1}{\rho_r}}{\frac{W_1}{\rho_r}+\frac{(W_2-W_1)}{\rho_s}} \quad (3)$$

where W_1 is de-swollen weight, W_2 is swollen weight, ρ_r is the density of rubber, and ρ_s is the density of toluene.

Based on the swelling equilibrium test, the extent of filler-matrix interactions between NR and filler was estimated by applying the Lorenz-Parks model [17], which can be expressed as follows,

$$\frac{Q_f}{Q_g} = ae^{-z}+b \quad (4)$$

where Q_f and Q_g refer to the amounts of absorbed solvent in filled and gum rubber vulcanizates, where a and b are constants, and z is the weight fraction of filler.

The Q values can be calculated as shown here [18].

$$Q = \frac{\text{Swollen wt. - Dried wt.}}{\text{Original wt.}} \quad (5)$$

Stress-strain behavior and tensile properties, including 100% modulus, 300% modulus, tensile strength, and elongation at break of crosslinked NR and its composites, were evaluated by using a universal tensile testing machine, LR5K Plus (LLOYD Instruments, UK). As per ISO 37 (type 2), the dumbbell-shaped specimens were cut, and the tensile characteristics were evaluated at a crosshead speed of 500 mm/min.

A scanning electron microscope (SEM), model Quanta 400 (Thermo Fisher Scientific, Czech Republic), was used to investigate the dispersion of different $CaCO_3$ fillers in the NR matrix. Before SEM analysis, the samples were sputter-coated with gold and cryogenically shattered using liquid nitrogen.

Measurements using wide-angle X-ray scattering (WAXS) were used to examine the microstructure alterations, i.e., the crystallinity changes that occurred during the stretching of the NR and its composites. The measurements were performed at Beamline 1.3W, the Siam Photon Laboratory, Synchrotron Light Research Institute (SLRI), Nakhon-Ratchasima, Thailand. The stretching tests were run at 50 mm/min crosshead speed. The data were processed using the SAXSIT software (version 4.63).

The degree of crystallinity during stretching was estimated using Equation 6 [19]:

$$\text{Degree of crystallinity (\%)} = \frac{A_{cr}}{A_{cr}+A_{am}} \quad (6)$$

where A_{cr} denotes the area below the (200) and (120) crystalline peaks, and A_{am} refers to the area for the amorphous halo.

The temperature scanning stress relaxation (TSSR) meter (Brabender, Duisburg, Germany) was used to assess the thermomechanical properties of NR composites under non-isothermal conditions. As per ISO527 (type 5A), the samples were cut into the shape of dumbbells. The samples were first pre-stretched to 50% strain at 23°C during testing, and they were kept at this condition for two hours. The samples were then heated at a steady rate of 2°C per minute until they broke as part of a non-isothermal stress relaxation test [20,21]. The TSSR parameters, including the temperatures at which the force has dropped by 50% and by 90% (T_{50} and T_{90}) from the initial force, and the TSSR index, were evaluated.

Results and Discussion

Table 2 illustrates the chemical compositions of eggshell and commercial-grade $CaCO_3$ powders. CaO was the primary ingredient in the commercial-grade $CaCO_3$ and eggshell powders. The highest content of CaO was found in the commercial grade $CaCO_3$ at about 55.76%. ESP 132 contains 53.07% of CaO, whereas the ESP 300 showed about 52.96% of CaO. This indicates that eggshell powder is a substitute $CaCO_3$ source and a potential filler for rubber products. Considering the amounts of some important metal oxides, namely MgO, SrO, Na_2O, K_2O, and Fe_2O_3 [6], it was found that the ESP 132

showed the highest content of these (~ 0.75%), while the commercial grade $CaCO_3$ showed the lowest total amount of these (~ 0.56%).

The two primary components discovered in all types of filler in the STA8000 test findings were the organic portion (i.e., CHNO) and CO_2. The CO_2 was the component obtained from burning $CaCO_3$ [6], and its amount was not significantly different by filler. On the other hand, compared to commercial-grade $CaCO_3$, the eggshell powder had a higher organic content. This difference in organic part was attributed to the treatment of commercial-grade $CaCO_3$ as reported in [13], while protein remained in the eggshell powders ESP 132 and ESP 300 [6].

Figure 2 displays torque time curves during vulcanization for all composites loaded with various $CaCO_3$ types. For reference, the filler-free sample (Control) was also included. The vulcanization parameters M_L, M_H, $M_H - M_L$, t_{s1}, $t_{90,}$ and CRI are listed in Table 3. Regardless of the type and particle size of filler, the M_L and M_H were found to increase with the addition of filler. The inflexible properties of fillers enhance stiffness and diminish the mobility of rubber chains, increasing the viscosity of the compounds and generally impeding the flow of rubber compounds [22]. Compared to the Ref - $CaCO_3$ composite, the ES - $CaCO_3$ composites showed higher M_L and M_H. The greater M_L suggested that the composites containing eggshell filler would give more difficulty in processing than the composites filled with commercial-grade $CaCO_3$. On the other hand, the fully vulcanized ES-$CaCO_3$ composite samples' greater stiffness or shear modulus was indicated by the bigger M_H.

Table 2. Characteristics of commercial grade $CaCO_3$, ESP 132 and ESP 300

Testing technique	Ingredient	Volume (%)		
		Commercial $CaCO_3$	ESP 132	ESP 300
XRF	CaO	55.76	53.07	52.96
	Total metal oxide, i.e., Na_2O, MgO, K_2O, Fe_2O_3, SrO	0.56	0.75	0.74
STA8000	CHNO	0.50	3.01	3.46
	CO_2	42.73	42.52	42.27

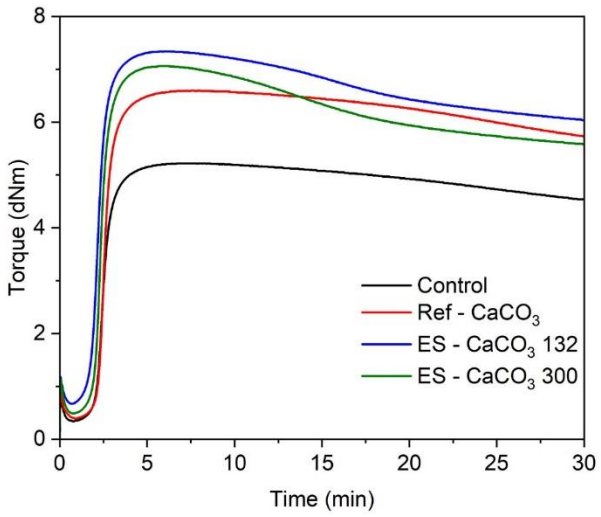


Figure 2. Curing characteristics of NR compounds containing various fillers at 30 phr with gum rubber as control baseline

Table 3. Curing parameters including M_L, M_H, $M_H - M_L$, t_{s1}, $t_{90,}$ and CRI

Sample	Cure Characteristic					
	M_L (dNm)	**M_H (dNm)**	**$M_H - M_L$ (dNm)**	**t_{s1} (min)**	**t_{90} (min)**	**CRI (/min)**
Control	0.34±0.00	5.22±0.00	4.88±0.00	2.22±0.01	3.35±0.01	88.50±1.13
Ref - $CaCO_3$	0.39±0.06	6.60±0.06	6.21±0.12	2.27±0.24	3.42±0.33	86.96±7.16
ES - $CaCO_3$ 132	0.67±0.00	7.34±0.00	6.67±0.00	1.85±0.01	2.97±0.00	89.29±0.56
ES - $CaCO_3$ 300	0.49±0.02	7.06±0.03	6.57±0.05	2.05±0.07	3.12±0.02	93.46±4.63

When filler was added, the $M_H - M_L$ rose as well. The composites filled with eggshell powder had the highest $M_H - M_L$, whereas commercial-grade $CaCO_3$ produced a lower value. Usually, $M_H - M_L$ correlates with crosslink density in the composite [23,24]. Compared to the Ref-$CaCO_3$ sample, a higher $M_H - M_L$ in the composites containing eggshell filler denotes a higher crosslink density. Moreover, the t_{s1} refers to the induction time before the vulcanization reaction starts, and t_{90} refers to the cure time where the torque reaches 90% of the optimum point. Both t_{s1} and t_{90} of the composites filled with eggshell powder decreased upon the addition of filler compared to the Ref-$CaCO_3$ composite sample, suggesting the faster curing reaction occurred in the composites containing eggshell powder. The higher CRI values compared to the control and Ref-$CaCO_3$ samples validated the eggshell powder-containing sample's quicker curing process. The greater crosslink density formation with shorter t_{s1} and t_{90} in the composites containing eggshell powder was attributed to both metal oxide and protein constituents (see **Table 2**). It has been discovered that the metal oxide and protein found in eggshell powder may contribute to the curing process, enhancing the vulcanization reaction's effectiveness [6, 25, 26]. This would affect the composites' modulus, cure rate, and crosslink density. The ES-$CaCO_3$ 132 sample showed the lowest values of t_{s1} and t_{90}, possibly due to the highest amount of metal oxides.

Figure 3 shows SEM images of filler dispersion in the rubber composites filled with commercial-grade $CaCO_3$ or with eggshell powder. The commercial-grade $CaCO_3$ exhibited comparatively more uniform dispersion in the matrix (**Figure 3a**) as compared to the eggshell powder, but the composites filled with eggshell powder had less uniform dispersions (**Figures 3b and 3c**). The average aggregate size of filler in the Ref-$CaCO_3$ sample measured by using Image J software was about 0.66 ± 0.17 µm, while the sizes of filler in the ES - $CaCO_3$ 132 and ES - $CaCO_3$ 300 were about 0.73 ± 0.33 µm and 0.77 ± 0.36 µm, respectively.

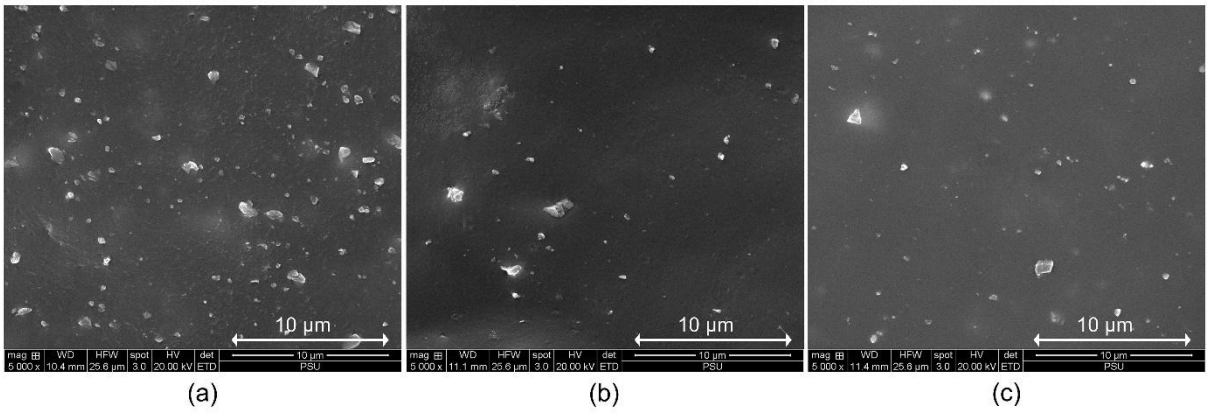


Figure 3. SEM images of the various NR composites, (a) Ref-$CaCO_3$, (b) ES-$CaCO_3$ 132, and (c) ES-$CaCO_3$ 300

Interestingly, the sizes of eggshell powder dispersed in the ES-$CaCO_3$ 132 and ES-$CaCO_3$ 300 samples differed slightly from the Ref-$CaCO_3$ sample, despite their initial particle sizes being very different. After sieving, the sizes of eggshell powder particles were approximately 132 µm and 300 µm, whereas the particle size of commercial-grade $CaCO_3$ was approximately 2.1 µm. The results clearly suggest that the initial size of eggshell filler does not affect the final dispersion in the rubber

matrix due to the high shear force generated during mixing, which caused the filler break down to smaller size (~1 μm). Because the smaller filler particles scattered throughout the rubber matrix have a wider surface area and may interact with the rubber more effectively, a reduction in filler size would improve the final characteristics of the rubber composite [27]. The surface treatment of commercial-grade $CaCO_3$ is responsible for its more homogeneous dispersion and smaller particle size. The surface treatment enhanced the dispersion and made it possible for the particles to stick firmly to the rubber matrix. The dispersions of eggshell powders, ES-$CaCO_3$ 132 and ES-$CaCO_3$ 300, were not significantly different from each other, but were poorer than that of the Ref-$CaCO_3$, because the eggshell powders had no surface treatment.

Figure 4 shows the effects of the various fillers on the swelling of the NR composites. In general, the fillers decreased the degree of NR swelling, indicating that the addition of filler decreased the toluene solvent's penetration into the rubber composite.

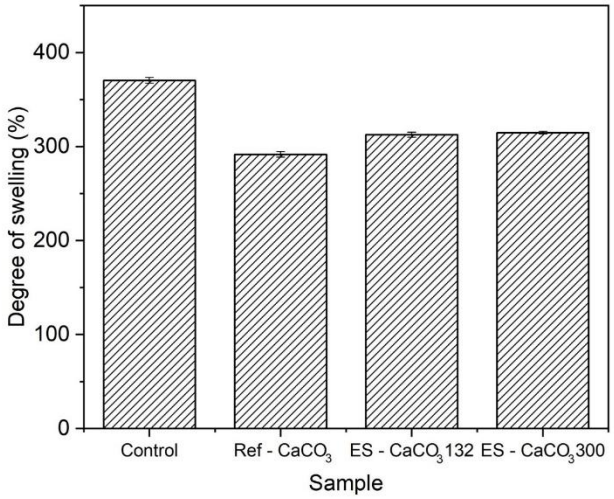


Figure 4. Swelling characteristics of NR composites containing various fillers

Because the fillers acted as a barrier to prevent solvent penetration into the rubber composite, the degree of swelling was decreased. Compared to the composites with eggshell filler, the Ref-$CaCO_3$ composite swelled less. This was explained by the commercial-grade $CaCO_3$'s improved dispersion in the rubber matrix, as previously observed. A larger surface area for interaction between the filler and rubber matrix was made possible by the filler's smaller size and more uniform distribution. As a result, the rubber matrix was better protected from toluene solvent penetration. On the other hand, poorer filler dispersion of the eggshell powder resulted in a lower interaction with the matrix, reducing the bonding between the filler and rubber, causing a comparative increase in swelling.

Figure 5 shows the total crosslink densities in NR composites filled with the alternative types of $CaCO_3$. In general, the degree of swelling is inversely correlated with the overall crosslink density; a higher crosslink density is indicated by a lower degree of swelling [28]. According to **Figure 5**, adding filler raised the composites' overall crosslink density. Since some rubber chains were absorbed on the filler surfaces, forming pseudo-crosslinking sites, the total crosslink density was increased. The total crosslink densities of the ES - $CaCO_3$ 132 and ES-$CaCO_3$ 300 were lower than that of the Ref-$CaCO_3$ due to nonuniform dispersion with slightly larger particle size of eggshell filler in the rubber matrix. Poorer dispersion led to weaker interactions between the filler and the rubber, lowering the crosslink density.

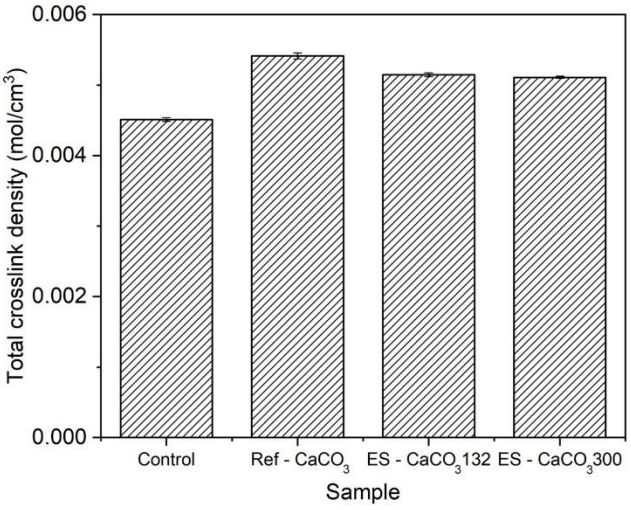


Figure 5. Total crosslink densities of NR composites containing the various types of filler

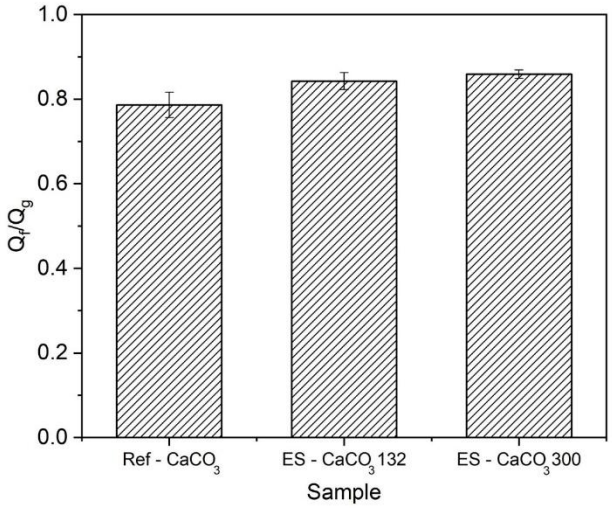


Figure 6. Rubber-filler interactions in NR composites containing various types of fillers

It should be noted that the torque trend discovered in rheometric testing was different from the crosslink density trend acquired from the swelling test. The Ref-$CaCO_3$ showed the greatest crosslink density in the swelling test, while the ES-$CaCO_3$ 132 showed the greatest crosslink density inferred from the curing test based on $M_H - M_L$. The different test conditions may explain this difference. The $M_H - M_L$ differences are attributed to chemical interactions, i.e., chemical cross-links between rubber chains, since the test was conducted at a higher temperature. Both chemical and physical crosslinks, such as chain entanglements and filler–rubber interactions, were included in the room temperature swelling test [4, 29]. Strong rubber-filler bonding may have an impact on the apparent crosslink density determined by a swelling test [30, 31]. The swelling test findings showed that the Ref-$CaCO_3$ composites had more filler-rubber interactions than the ES-$CaCO_3$ composites.

The Lorenz–Park model was used to assess the degree of interactions between rubber and filler to further validate the interaction between phases [17]. **Figure 6** shows the variation of the interaction parameter (Q_f/Q_g) of the NR composites filled with commercial-grade $CaCO_3$ and eggshell powder. According to the Lorenz–Park model, a lower Q_f/Q_g

indicates stronger rubber-filler interactions [4, 32]. Among the different composites, the lowest Q_f/Q_g was seen in the Ref-$CaCO_3$, while the composites filled with eggshell showed a higher Q_f/Q_g. The smaller agglomeration size of the filler in the rubber matrix was thought to be the reason for the greater interactions between rubber and commercial-grade $CaCO_3$. The ES-$CaCO_3$ 132 showed slightly lower Q_f/Q_g than the ES-$CaCO_3$ 300, possibly due to a slightly better dispersion. The Q_f/Q_g results confirmed that the greatest interactions between rubber and filler were achieved in the Ref-$CaCO_3$ case, while the least were in the ES-$CaCO_3$ 300 case.

Figure 7 shows representative stress-strain curves of the Ref-$CaCO_3$, ES-$CaCO_3$ 132, and ES-$CaCO_3$ 300. The averages of 100% modulus, 300% modulus, tensile strength, and elongation at break are summarized in **Table 4**. Depending on the kind of $CaCO_3$ used, the tensile characteristics were impacted by either eggshell or commercial-grade $CaCO_3$. The rubber composites' modulus was increased by all forms of $CaCO_3$, especially the 300% modulus. The rubber chains become less mobile when fillers are added to the rubber matrix, which raises the rubber composite's modulus [33]. The tensile strength and elongation at break of the Ref-$CaCO_3$ decreased slightly compared to the control sample, whereas a greater reduction in both properties was noticed in the ES-$CaCO_3$ composites. Considering the composites filled with eggshell powder, the tensile strength and elongation at break remain relatively high, i.e., 17.83 MPa and 394% strain in the ES-$CaCO_3$ 132, and a drastic reduction of the tensile strength was observed in the ES-$CaCO_3$ 300 case to 12.71 MPa. The changes in tensile properties can be explained by the Q_f/Q_g ratios in **Figure 6**.

The inclusion of filler in the rubber matrix may have contributed to a minor decrease in the characteristics of Ref-$CaCO_3$ when compared to the unfilled control. In contrast to the eggshell powder, the surface treatment of the commercial-grade $CaCO_3$ promoted greater interfacial adhesion and filler-rubber interactions by improving compatibility between the filler and rubber matrix. Therefore, the Ref - $CaCO_3$ can withstand tensile forces more effectively than the other filled cases. Because of lower interactions with the rubber matrix, the addition of eggshell powder decreased the tensile strength and elongation at break. Although the tensile properties of the ES - $CaCO_3$ 132 were lower than those of the Ref - $CaCO_3$, its 100% and 300% moduli, tensile strength, and elongation at break remained relatively high, with tensile strength ~ 17 MPa and elongation at break ~ 400%. Thus, it seems possible to use this candidate filler in various goods made of rubber. In addition to being a bio-filler, it is plentiful and renewable, both of which are important benefits for the rubber sector.

The hardness of rubber was also increased with the incorporation of fillers (see **Table 4**). This resulted from the fact that adding filler makes materials more rigid. But the variance in fillers did not substantially impact the hardness.

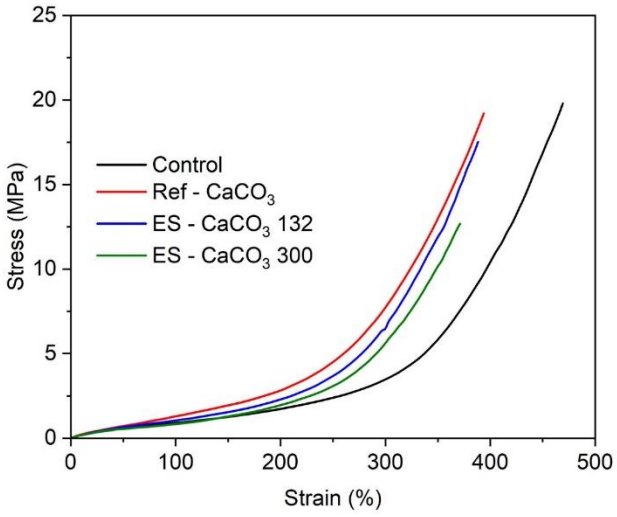


Figure 7. Representative stress-strain curves of NR composites containing various types of filler

Table 4. 100% modulus (100% mod), 300% modulus (300% mod), tensile strength, elongation at break, and hardness for the NR composites

Sample	Properties				
	100% Mod (MPa)	**300% Mod (MPa)**	**Tensile Strength (MPa)**	**Elongation at Break (%)**	**Hardness (Shore A)**
Control	0.93±0.06	3.96±0.67	19.89±0.88	470±40	34.78±0.44
Ref - $CaCO_3$	1.24±0.13	7.90±0.35	19.22±0.64	412±34	39.11±0.33
ES - $CaCO_3$ 132	1.06±0.04	6.38±0.00	17.83±0.68	394±5	40.00±0.00
ES - $CaCO_3$ 300	0.92±0.06	6.18±0.68	12.71±0.58	361±10	40.56±0.53

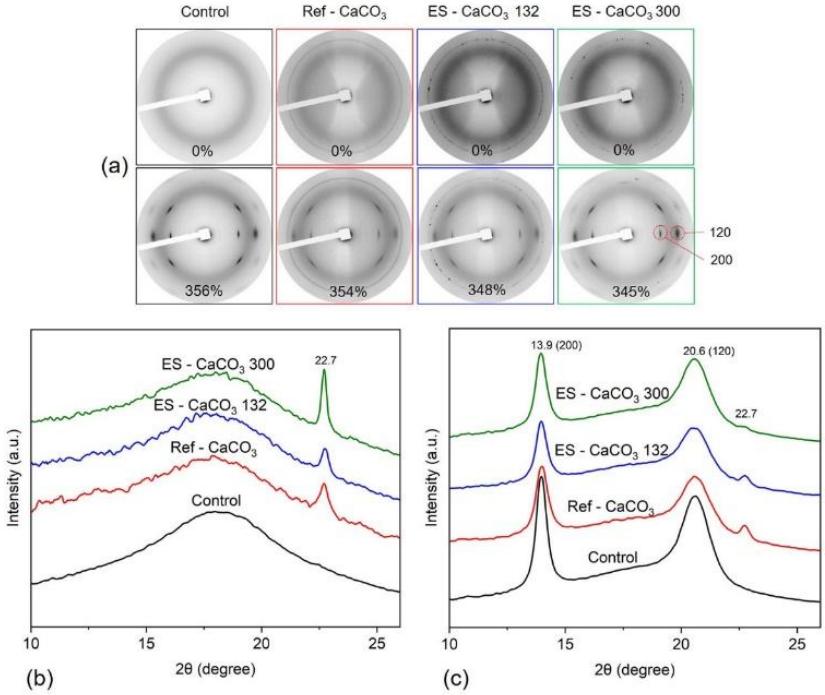


Figure 8. (a) Two-dimensional (2D) WAXS images of the various samples at 0% strain and at a high strain (i.e., ~350%), and the corresponding 1D WAXS patterns at (b) 0% strain, and (c) at high strain

WAXS was used to determine how filler addition affected the NR's strain-induced crystallization. **Figure 8(a)** shows two-dimensional (2D) WAXS images of the various samples before (0% strain) and after deformation to 345% - 356% strains. Their corresponding 1D patterns are included in **Figures 8(b) and 8(c)**. As can be seen from **Figure 8(a)**, the 2D WAXS images of the control sample showed no reflection spots at the stage before deformation starts (at 0% strain), while all the composites showed a ring-shaped reflection attributed to $CaCO_3$ [34]. The corresponding 1D pattern of the control sample shown in **Figure 8(b)** showed only an amorphous halo without any diffraction peaks because there was no strain-induced crystallization before deformation. However, the 1D patterns of all composites showed a diffraction peak at 2θ of 22.7° (see **Figure 2(b)**), due to the crystalline peak of the $CaCO_3$ [6]. After stretching the samples up to strains of about 345%-356%, the 2D images of all samples (**Figure 8(a)**) clearly showed various reflection spots in different positions due to the stretching has caused molecular chain orientation and strain-induced crystallization [35]. Even at a high stretching level, the composites continued to exhibit ring-shaped reflections. These ring-shaped reflections showed that the filler was not aligned during rubber deformation [34]. The most interesting reflection sites are the crystallographic planes (200) and (120), which are indicated by red circles. As shown in **Figure 8(c)**, the crystallographic planes (200) showed the diffraction peaks at 2θ of about 14° while the (200) planes showed at 2θ of about 21° [36]. Since the crystalline

peak of $CaCO_3$ was seen at 2θ of 22.7°; thus, it would surely not interfere with observing the crystallization of NR at 2θ of 14° and 21°. By adding fillers, the height and area under diffraction peaks at 14° and 21° decreased. This implies that strain-induced crystallization was delayed by the filler. Neither eggshell nor commercial-grade $CaCO_3$ functions as an NR crystallization nucleating agent.

Figure 9 illustrates how crystallinity for the NR and NR composite samples depends on strain. Since stretching was the source of crystallization in the NR, the crystallinity in every instance increased with strain [37]. The composites' crystallinity was lower than that of the control at the same strain, indicating that the fillers did not act as a nucleation agent for strain-induced crystallization.

Figure 10 shows normalized force curves during non-isothermal relaxation of the NR and its composites. Three stages were visible in the normalized force curves. An entropy effect was identified as the cause of a modest rise in the normalized force in the temperature range of 30 to 50 °C [38], normalized force decreased between 50 and 100 °C as a result of the physical bonds between rubber molecules or between rubber and filler being broken [22], and a substantial reduction in force beyond 120 °C was attributable to the cleavage of cross-links between rubber chains in temperature range 90-160 °C and chain scission at 160-220 °C [39]. The raw data obtained from the TSSR measurements, including the temperatures at which the force has dropped by 50% and 90% (T_{50} and T_{90}) from the initial force, and the TSSR index, are summarized in **Table 5**.

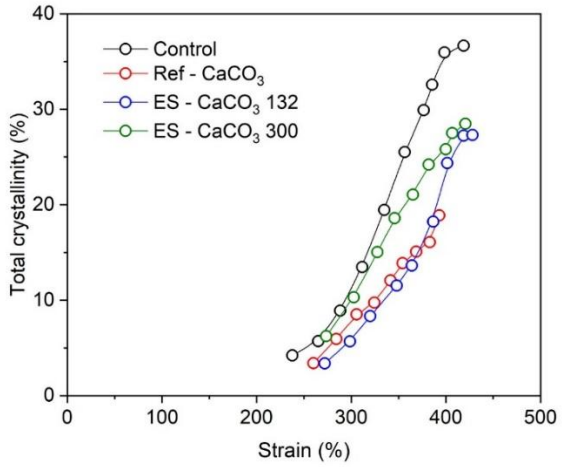


Figure 9. Variation of crystallinity with strain for the NR composites containing various types of filler

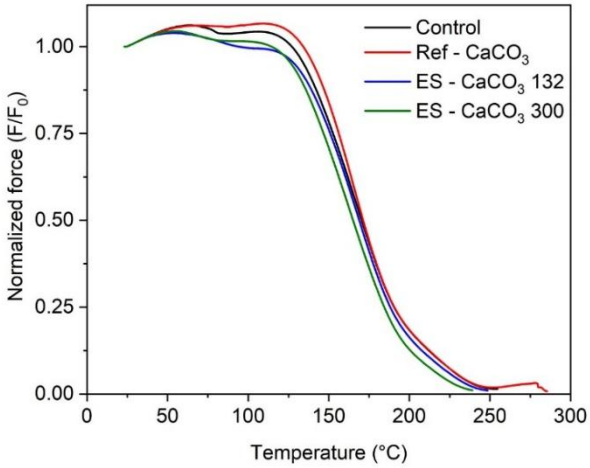


Figure 10. Normalized force during non-isothermal relaxation of NR composites containing various types of fillers

Table 5. Temperatures at which the force has dropped by 50%, and 90% (T_{50} and T_{90}), and the TSSR index for the NR composites containing various types of filler

Parameter \ Sample	Control	Ref - $CaCO_3$	ES - $CaCO_3$ 132	ES - $CaCO_3$ 300
T_{50} [°C]	170.4	171.3	168.9	165.1
T_{90} [°C]	218.0	218.3	213.9	206.2
TSSR-Index [-]	0.80	0.82	0.80	0.79

The T_{50} is commonly used to indicate the upper limit of service temperature for the tested materials, and the T_{90} is used for predicting material stability [40, 41]. The material's rubber-like behavior was shown by the TSSR indices, which were effectively estimated from the region below the normalized force-temperature curve (**Figure 10**) in accordance with the following relationship [21].

$$\text{TSSR index} = \frac{\int_{T_0}^{T_{90}} F(T)/F_0 dT}{T_{90}-T_0} \quad (7)$$

Here, F and F_0 are the forces at temperature T and at starting temperature T_0, respectively.

According to **Figure 10** and **Table 5**, the addition of commercial-grade $CaCO_3$ raised the normalized force across the measured temperature range, and this composite's T_{50}, T_{90}, and TSSR index were greater than those of the control, but the addition of eggshell powder revealed a different pattern. Increases in normalized force, T_{50}, T_{90}, and the TSSR index of the Ref-$CaCO_3$ revealed significant interactions between the commercial-grade $CaCO_3$ and the NR matrix, indicating that this improvement was caused by good dispersion of commercial-grade $CaCO_3$ with great rubber-filler contact. Conversely, a reduction in those values is seen for both the ES-$CaCO_3$ 132 and the ES-$CaCO_3$ 300, indicating comparatively poorer interactions between eggshell and NR. Although the T_{50} and T_{90} of the NR composites were decreased on inclusion of eggshell powder, the TSSR indexes of these composites remained comparable to the control sample, suggesting that eggshell powder may not be appropriate when thermal resistance is pursued.

According to the study's findings, adding filler generated from eggshell waste to NR composites is very desirable. Although the addition of eggshell powder resulted in poor thermal properties, the mechanical properties remained relatively high, particularly in the ESP 132 case. Thus, the use of eggshell waste as filler in NR appears practical.

Conclusion

In this study, NR and NR composites filled with eggshell powder were developed. For reference, a composite of commercial-grade $CaCO_3$ was also prepared. The inclusion of eggshell powder improved the rubber composites' curing torque, swelling resistance, crosslink density, and modulus at different stresses when compared to the unfilled control sample, but the tensile strength, extensibility, and thermomechanical qualities were found to be negatively impacted. However, compared to eggshell powder, the inclusion of commercial-grade $CaCO_3$ enhanced all attributes because of the greater filler dispersion generated by more interactions with the rubber matrix. The crystallization of NR during stretching was not improved by any of the tested fillers, so these fillers did not serve as nucleating agents for NR crystallization. The tensile strength of NR composites filled with ESP 132 decreased by 7.23% compared to that filled with commercial-grade $CaCO_3$, while a greater reduction of 33.87% was observed for the composite containing ESP 300. Although the eggshell powder as filler resulted in poor thermal properties, the mechanical properties remained relatively high, with tensile strength ~ 17.83 MPa and elongation at break ~ 394%, particularly in the case of ESP 132. Therefore, it seems practical to utilize eggshell waste as filler in goods made of rubber. Besides being a bio-filler, it is abundant and renewable, which are significant advantages for a rubber formulation.

Future research should focus on optimizing the dispersion of eggshell powder within the rubber matrix through surface modification or the application of coupling agents. In addition, long-term properties such as aging, fatigue, and environmental resistance tests under industrially relevant conditions are recommended to further assess the suitability of eggshell-filled NR composites for industrial applications.

References

1. El Mogy, S. A., Darwish, N. A. and Awad, A. (2020). Comparative study of the cure characteristics and mechanical properties of natural rubber filled with different calcium carbonate resources. *Journal of Vinyl and Additive Technology,* 26 (3): 309 – 315.
2. Ramesh, M., Rajeshkumar, L. N., Srinivasan, N., Kumar, D. V. and Balaji, D. (2022). Influence of filler material on properties of fiber-reinforced polymer composites: a review. *e-Polymers,* 22 (1): 898 – 916.
3. Sowinska-Baranowska, A. and Maciejewska,

M. (2023). Potential utilization of ground eggshells as a biofiller for natural rubber biocomposites. *Materials,* 16 (8): 2988.
4. Hayeemasae, N., Soontaranon, S. and Masa, A. (2024). Comparative investigation of nano-sized silica and micrometer-sized calcium carbonate on structure and properties of natural rubber composites. *Polymers,* 16 (8): 1051.
5. Damircheli, M., MajidiRad, A. and Asmatulu, R. (2025). Calcium carbonate nanoparticle-reinforced rubber: enhancing dynamic mechanical performance and thermal properties. *Journal of Materials Research and Technology,* 36: 326–336.
6. Intharapat, P., Kongnoo, A. and Kateungngan, K. (2013). The potential of chicken eggshell waste as a bio-filler filled epoxidized natural rubber (ENR) composite and its properties. *Journal of Polymers and the Environment,* 21 (1): 245–258.
7. Bashir, A. S., Manusamy, Y., Chew, T. L., Ismail, H. and Ramasamy, S. (2017). Mechanical, thermal, and morphological properties of eggshell powder-filled natural rubber latex foam. *Journal of Vinyl and Additive Technology,* 23 91): 3 – 12.
8. Munusamy, Y. and Kchaou, M. (2023). Usage of eggshell as potential bio-filler for acrylonitrile butadiene rubber (NBR) latex film for glove applications. *Ain Shams Engineering Journal,* 14 (11): 102512.
9. Kowshik, S., Sharma, S., Rao, S., Shettar, M. and Hiremath, P. (2023). Mechanical properties of post-cured eggshell-filled glass-fibre-reinforced polymer composites. *Journal of Composites Science,* 7 (2): 49.
10. Tangboriboon, N., Pannangpetch, W., Aranyik, K., Petcharoen, K. and Sirivat, A. (2015). Embedded eggshells as a bio-filler in natural rubber for thermal insulation composite foams. *Progress in Rubber, Plastics and Recycling Technology,* 31 93): 189 – 205.
11. Bhagavatheswaran, E. S., Das, A., Rastin, H., Saeidi, Hoda, Jafari, S. H., Vahabi, H., Najafi, F., Khonakdar, H. A., Formela, K., Jouyandeh, M., Zarrintaj, P. and Saeb, M. R. (2019). The taste of waste: the edge of eggshell over calcium carbonate in acrylonitrile butadiene rubber. *Journal of Polymers and the Environment,* 27: 2478 – 2489.
12. Barrera, C. S. and Cornish, K. (2015). Novel mineral and organic materials from agro-industrial residues as fillers for natural rubber. *Journal of Polymers and the Environment,* 23 (4): 437 – 448.
13. Manaila, E., Craciun, G., Ighigeanu, D., Lungu, I. B., Dumitru Grivei, M. D. and Stelescu, M. D. (2022). Degradation by electron beam irradiation of some composites based on natural rubber reinforced with mineral and organic fillers. *International Journal of Molecular Sciences,* 23(13), 6925.
14. Lumlong, S., Pungpo, P., Khamsri, B., Saenglam, I. and Kongkaew, C. (2018). Study the effect of calcium carbonate from eggshell as a filler in natural rubber. *International Journal of Advanced Science, Engineering and Technology,* 6 (1): 12 – 15.
15. Flory, P. J. and Rehner, J. Jr. (1943). Statistical mechanics of crosslinked polymer networks I. Rubberlike elasticity. *Journal of Chemical Physics,* 11 (11): 512 – 520.
16. Musto, S., Barbera, V., Cipolletti, V., Citterio, A. and Galimberti, M. (2017). Master curves for the sulphur assisted crosslinking reaction of natural rubber in the presence of nano- and nano-structured sp^2 carbon allotropes. *eXPRESS Polymer Letters,* 11 (6): 435 – 448.
17. Lorenz, O. and Parks, C. R. (1961). The crosslinking efficiency of some vulcanizing agents in natural rubber. *Journal of Polymer Science,* 50 (154): 29 9– 312.
18. Swapna, V. P., Stephen, R., Greeshma, T., Sharan Dev, C. and Sreekala, M. S. (2016). Mechanical and swelling behavior of green nanocomposites of natural rubber latex and tubular shaped halloysite nanoclay. *Polymer Composites,* 37 (2): 602 – 611.
19. Hayeemasae, N., Soontaranon, S. and Masa, A. (2024). Influences of compatibilizer type and loading on properties of phenolic resin-crosslinked natural rubber composites filled with sepiolite. *eXPRESS Polymer Letters,* 18 (11): 1135 – 1148.
20. Vennemann, N. and Fremuth, K. (2021). TSSR: a versatile test method for elastomers and TPEs. *Rubber Plastics News,* July 12: 14 – 17.
21. Chatterjee, T., Vennemann, N. and Naskar, K. (2018). Temperature scanning stress relaxation measurements: a unique perspective for evaluation of the thermomechanical behavior of shape memory polymer blends. *Journal of Applied Polymer Science,* 135 (2): 45680.
22. Pongdong, W., Kummerlowe, C., Vennemann, N., Thitithammawong, A. and Nakason, C. (2018). A comparative study of rice husk ash and siliceous earth as reinforcing fillers in epoxidized natural rubber composites. *Polymer Composites,* 39 (2): 414 – 426.
23. Rabiei, S. and Shojaei, A. (2016). Vulcanization kinetics and reversion behavior of natural rubber/styrene-butadiene rubber blend filled with nanodiamond–the role of sulfur curing system. *European Polymer Journal,* 81: 98 – 113.
24. Hayeemasae, N., Adair, A. and Masa, A. (2022). Comparative study on viscosities, stress relaxation, curing and mechanical properties of sepiolite and silica filled natural rubber composites. *Malaysian Journal of Analytical*

Sciences, 26, 176-190.

25. Wang, P. Y., Chen, Y. and Qian, H. L. (2007). Vulcanization kinetics of low-protein natural rubber with use of a vulcameter. *Journal of Applied Polymer Science,* 105 (6): 3255 – 3259.
26. Masa, A., Krem-ae, A., Ismail, H. and Hayeemasae, N. (2020). Possible use of sepiolite as alternative filler for natural rubber. *Materials Research,* 23: e20200100.
27. Chu, Q., Tian, X., Bian, H. and Wang, C. (2025). Optimization of mechanical and dynamic properties of tread rubber using fumed silica and hydration processing. *Polymers,* 17 (6): 714.
28. Masa, A., Soontaranon, S. and Hayeemasae, N. (2020). Influence of sulfur/accelerator ratio on tensile properties and structural inhomogeneity of natural rubber. *Polymer Korea,* 44 (4): 519–526.
29. Hayeemasae, N., Waesateh, K., Soontaranon, S. and Masa, A. (2022). Effect of vulcanization systems and crosslink density on tensile properties and network structure of natural rubber. *Jurnal Teknologi,* 84 (6): 181–187.
30. Salgueiro, W., Marzocca, A., Somoza, A., Consolati, G., Cerveny, S., Quasso, F. and Goyanes, S. (2004). Dependence of the network structure of cured styrene butadiene rubber on the sulphur content. *Polymer,* 45 (17): 6037 – 6044.
31. Thomas, D., Janardhanan, C. and Sebastian, M. T. (2011). Mechanically flexible butyl rubber–$SrTiO_3$ composite dielectrics for microwave applications. *International Journal of Applied Ceramic Technology,* 8 (5): 1099–1107.
32. Ismail, H., Omar, N. and Othman, N. (2011). Effect of carbon black loading on curing characteristics and mechanical properties of waste tyre dust/carbon black hybrid filler filled natural rubber compounds. *Journal of Applied Polymer Science,* 121 (2): 1143–1150.
33. Inphonlek, S., Bureewong, N., Kotchapradit, S., Ruksakulpiwat, Y. and Ruksakulpiwat, C. (2025). Synergistic effects of hybrid bio-fillers and modified natural rubber on natural rubber composite properties. *Polymers,* 17 (5): 632.
34. Poompradub, S., Tosaka, M., Kohjiya, S., Ikeda, Y., Toki, S., Sics, I. and Hsiao, B. S. (2005). Mechanism of strain-induced crystallization in filled and unfilled natural rubber vulcanizates. *Journal of Applied Physics,* 97 (10): 103529.
35. Wongvasana, B., Thongnuanchan, B., Masa, A., Saito, H., Sakai, T. and Lopattananon, N. (2023). Reinforcement behavior of chemically unmodified cellulose nanofiber in natural rubber nanocomposites. *Polymers,* 15 (5): 1274.
36. Masa, A., Hayeemasae, N., Soontaranon, S., Pisal, M. H. M. and Rasidi, M. S. M. (2021). Effect of stretching rate on tensile response and crystallization behavior of crosslinked natural rubber. *Malaysian Journal of Fundamental and Applied Sciences,* 17 (3): 217 – 225.
37. Hayeemasae, N., Soontaranon, S. and Masa, A. (2023). Influence of different vulcanizing agents on structures and properties of sepiolite-filled natural rubber composites. *eXPRESS Polymer Letters,* 17 (2): 181–195.
38. Promsung, R., Nakaramontri, Y., Uthaipan, N., Kummerlowe, C., Johns, J., Vennemann, N. and Kalkornsurapranee, E. (2021). Effects of protein contents in different natural rubber latex forms on the properties of natural rubber vulcanized with glutaraldehyde. *eXPRESS Polymer Letters,* 15 (4): 308 – 318.
39. Nakaramontri, Y., Kummerlowe, C., Vennemann, N., Wisunthorn, S., Pichaiyut, S. and Nakason, C. (2018). Effect of bis(triethoxysilylpropyl)tetrasulfide (TESPT) on properties of carbon nanotubes and conductive carbon black hybrid filler filled natural rubber nanocomposites. *eXPRESS Polymer Letters,* 12 (10): 867–884.
40. Hayeemasae, N., Fathurrohman, M. I. and Masa, A. (2023). Effects of maleic anhydride content on thermomechanical and mechanical properties of maleated natural rubber. *Polymer Korea,* 47 (5): 565 – 573.
41. Pongdong, W., Kummerlowe, C., Vennemann, N., Thitithammawong, A. and Nakason, C. (2018). A comparative investigation of rice husk ash and siliceous earth as reinforcing fillers in dynamically cured blends of epoxidized natural rubber (ENR) and thermoplastic polyurethane (TPU). *Journal of Polymers and the Environment,* 26 (3): 1145 – 1159.